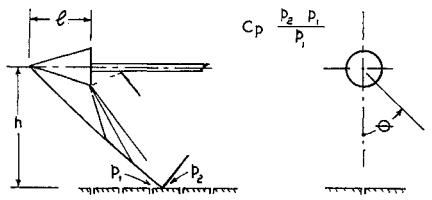

Fig 1 Layout of experiment

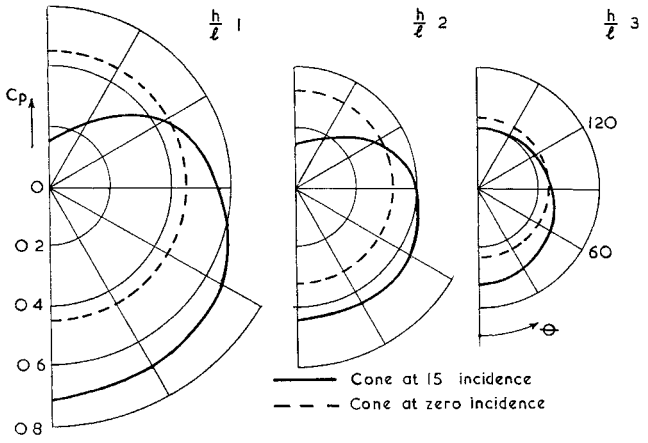

Fig 2 Shock strengths produced by 15 semiapex angle cone at $M = 2$

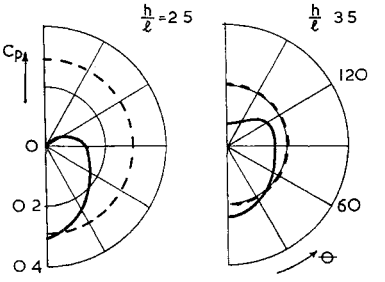

Fig 3 Comparison of shocks from slender delta and cone

riphery is again apparent, and, at large distances, this could cause the maximum shock strength from the wing to fall below the cone shock strength

The practical limitations imposed by the small size of the tunnel prevent definite conclusions being reached However, for at least as far from the body as it was possible to make measurements, there is a considerable circumferential evening up in the strength of the shock wave If this effect persists to larger distances, it is likely that the Walkden-Whitham approach, which neglects it, leads to a considerable overestimation of the sonic boom due to lift It is important to resolve this point, since the boom due to thickness or volume can be reduced or even virtually eliminated by interference, as in the Busemann biplane for wing thickness effects or the shrouded center body[5] for fuselage volume

References

[1] Rhyming, I L and Yoler, Y A, "Supersonic boom of wing-body configurations," J Aerospace Sci 28, 313–320 (1961)

[2] Morris, J, "An investigation of lifting effects on the intensity of sonic booms," J Roy Aeronaut Soc 64, 610–616 (1960)

[3] Walkden, F, "The shock pattern of a wing-body combination far from the flight path," Aeronaut Quart 9, 164 (May 1958)

[4] Whitham, G B, On the propagation of weak shock waves," J Fluid Mech 1, 290 (September 1956)

[5] Visich, M and Martellucci, A, "Theoretical and experimental analysis of a cowling as a means of a drag reduction for an axisymmetric center body," ARS J 29, 447–448 (1959)

Measurement of Droplet Size for Wide Range Particle Distributions

J H Roberts* and M J Webb†
Princeton University, Princeton, N J

A METHOD for the determination of a mean droplet diameter of a spray from the analysis of the small-forward-angle diffractively scattered light intensity as developed by Dobbins et al [1] was shown to be applicable only for certain limited types of droplet distributions These distributions were described by an upper-limit distribution function (ULDF) as proposed by Mugele and Evans[2] and were of a type having a preponderance of small droplets such as those commonly encountered in spray studies However, the occurrence of other distribution types in sprays and other polydispersions is not rare Thus it was of interest to investigate further the applicability of the diffractive-scattering measuring technique to distribution forms not included in the original work [1]

Because of the success of the ULDF in accurately describing actual distribution forms,[2] it was retained for study here The ULDF number distribution may be written, following the nomenclature of Ref 1, as

$$Nr(D) = C \frac{\exp -\{\delta \ln[aD/(D_\infty - D)]\}^2}{D^4(D_\infty - D)} \qquad (1)$$

where a and δ are shape parameters, D_∞ is the maximum droplet diameter in the distribution, and C is a constant, such that the probability for the occurrence of a droplet of diameter D in the interval $0 < D < D_\infty$ is unity Since the parameters a and δ give no easy physical interpretation for the resulting distribution form, two different parameters are used, as selected by Deiss,[3] which do yield simple geometric interpretation for the ULDF The two new parameters are the skewness factor $\bar{D}/D_\infty$ and the nondimensional half width $Q = X/\bar{D}$, where $\bar{D}$ is the most probable diameter in the distribution and X is the width of the function at the two diameters where frequency is half that of $\bar{D}$ These two diameters are designated $D + \frac{1}{2}$ and $D - \frac{1}{2}$

The conditions at $\bar{D}$ are determined from Eq (1) by differentiating with respect to D and setting the result equal to zero, which yields the following transcendental equation:

$$a = \left(\frac{D_\infty}{\bar{D}} - 1\right) \exp\left[\frac{1}{\delta^2}\left(\frac{5}{2}\frac{\bar{D}}{D_\infty} - 2\right)\right] \qquad (2)$$

Values of $D \pm \frac{1}{2}$ are derived by simply equating

$$\tfrac{1}{2}Nr(\bar{D}) = Nr(D \pm \tfrac{1}{2})$$

which yields a second transcendental equation of the form

$$\left(\frac{D \pm \frac{1}{2}}{\bar{D}}\right)^4 \frac{D_\infty - D \pm \frac{1}{2}}{D_\infty - \bar{D}} = 2 \exp -\delta^2 \left[\left(\ln \frac{aD \pm \frac{1}{2}}{D_\infty - D \pm \frac{1}{2}}\right) - \left(\ln \frac{a\bar{D}}{D_\infty - \bar{D}}\right)^2\right] \qquad (3)$$

Received December 6, 1963 This work was supported by the Air Force through its Office of Scientific Research on Grant 62 90

* Undergraduate; presently Analytical Engineer, Advanced Gas Turbine Applications Group, Pratt and Whitney, Division of United Aircraft Corporation

† Research Staff Member, Department of Aerospace and Mechanical Sciences

Table 1 Distributions selected for computation of mean illumination profile

$\bar{D}/D_\infty$	Q	a	δ
	0 501	1 182	2 13
0 4	0 741	0 905	1 52
	0 986	0 775	1 24
	1 226	0 625	1 083
	0 59	0 74	1 58
	0 97	0 54	1 10
0 5	1 38	0.395	0 90
	0 80	0 465	1 20
0 6	0 55	0 520	1 41
	0 96	0 400	0 985
	0 77	0 250	0 90
0 8	0 92	0 250	0 85
	1 00	0 250	0 80

Although distributions having the required form may easily be chosen from selected values of the geometric parameters ($\bar{D}/D_\infty$, Q), transposing to the mathematical parameters (a,δ) is not readily accomplished because of the emergence of the foregoing transcendental equations In order to facilitate these transpositions, graphs have been constructed[4] relating $\bar{D}/D_\infty$ and Q to a and δ, using $D_{32}/\bar{D}$ as a common reference parameter (Figs 1-3) The choice of $D_{32}/\bar{D}$, the volume-to-surface mean diameter for the distribution, as a reference parameter is a consequence of the findings of Ref 1 and will again be more apparent later

The forward light-scattering illumination profile resulting from a chosen droplet distribution form is calculated from the following equation of Ref 1:

$$I(\theta) = \frac{\int_0^{\zeta_\infty} \left[\frac{2J_1(\alpha_0\zeta)}{\alpha_0\zeta}\right]^2 \frac{\zeta_\infty}{\zeta_\infty - \zeta} \exp -\left(\delta \ln \frac{a\zeta}{\zeta_\infty - \zeta}\right)^2 d\zeta}{\int_0^{\zeta_\infty} \frac{\zeta_\infty}{\zeta_\infty - \zeta} \exp -\left(\delta \ln \frac{a\zeta}{\zeta_\infty - \zeta}\right)^2 d\zeta} \quad (4)$$

where $\zeta = D/D_0$, $\alpha_0 = \pi D_0\theta/\lambda$, and D_0 is any convenient dimension, such as $\bar{D}$ or D_{32}, θ is the scattering angle, and λ is the wavelength of the incident beam

Distribution forms selected here for investigation cover a range of skewness of $\bar{D}/D_\infty$ = 0 4, 0 5, 0 6, and 0 8 and various Q (Reference 1 dealt with cases for 0 13 < $\bar{D}/D_\infty$ <

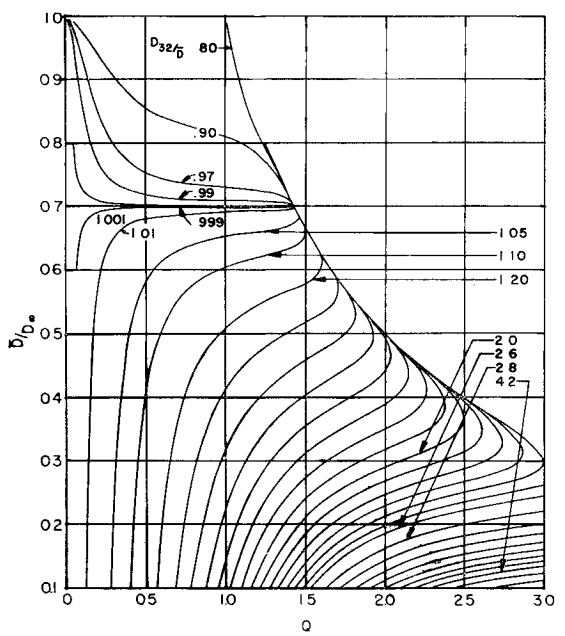

Fig 1 $\bar{D}/D_\infty$ vs Q for selected values of $D_{32}/\bar{D}$

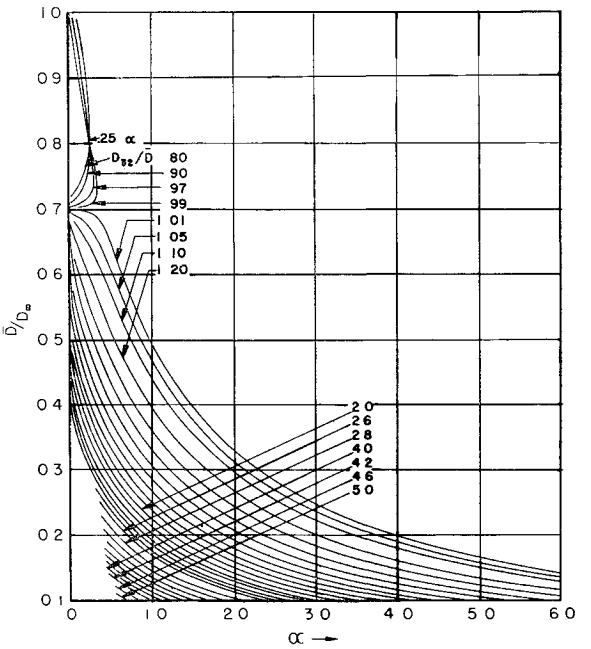

Fig 2 Values of $\bar{D}/D_\infty$ vs α for selected values of $D_{32}/\bar{D}$

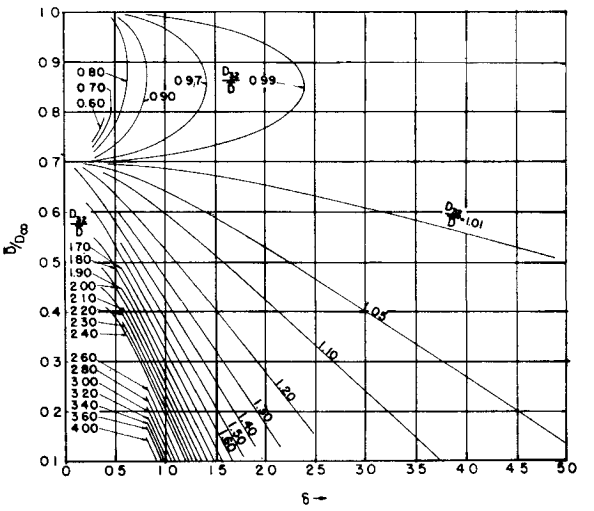

Fig 3 Values of $\bar{D}/D_\infty$ vs δ for selected values of $D_{32}/\bar{D}$

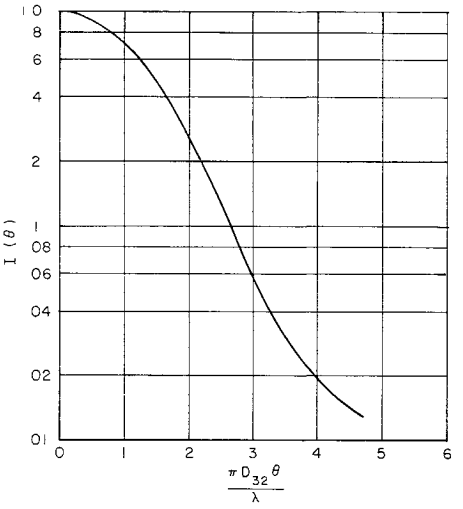

Fig 4 Mean theoretical illumination profile for all distributions investigated

Table 2 Mean theoretical illumination profile for 31 polydispersions obeying the ULDF

Reduced angle $\pi D_{32}\theta/\lambda$	Mean illumination $I(\theta)$	Standard deviation from mean $\pi D_{32}\theta/\lambda$ as a percentage of mean value
0	1 00	0
0 484	$9\ 20 \times 10^{-1}$	7 11
1 014	$7\ 00 \times 10^{-1}$	6 76
1 631	$4\ 00 \times 10^{-1}$	5 58
2 176	$2\ 00 \times 10^{-1}$	3 83
2 647	$1\ 00 \times 10^{-1}$	1 74
2 992	$6\ 00 \times 10^{-2}$	1 41
3 540	$3\ 00 \times 10^{-2}$	4 44
3 977	$2\ 00 \times 10^{-2}$	5 78
4 696	$1\ 30 \times 10^{-2}$	4 48

0 28) Using Figs 1-3, appropriate values of a and δ were determined for use in Eq (4) Values of Q were chosen to encompass both wide and narrow distributions However, values of Q which resulted in distributions that were sufficiently narrow as to approach a monodispersion, as characterized by distinct diffraction rings occurring in the corresponding illumination profile, were not included, as they would easily be distinguished as a monodispersion in an actual experimental measurement The actual values of the parameters for the distributions chosen are given in Table 1

As in the original work,[1] it was found subsequently[4] that when D_0 was set equal to D_{32} the various illumination profiles for all the distributions in Table 1 were almost coincident for values of $I(\theta)$ to 0 01 Furthermore, the mean curve for all the cases considered was very nearly coincident with the mean curve obtained for distributions having $0\ 13 < \bar{D}/D_\infty < 0\ 28$ [1] This result naturally led to an investigation of the complete range of distributions (i e , $0\ 13 < \bar{D}/D_\infty < 0\ 8$) with a determination of the mean curve for $I(\theta)$ vs $\pi D_{32}\theta/\lambda$ and the percent standard deviation from the mean for a total of 31 different distributions (18 from Ref 1, and 13 here) These results are tabulated in Table 2 and the mean curve plotted in Fig 4

In fitting an experimentally determined illumination profile to the curve of Fig 4, an obvious choice for determining D_{32} is in the region of $I(\theta) = 8 \times 10^{-2}$, where the standard deviation is only slightly greater than 1% The close coincidence of all the theoretical illumination profiles in this region is a consequence of the occurence of discreet diffraction rings for monodispersions, the first ring occurring at $\pi D_{32}\theta/\lambda = 3\ 83$ Although no distributions selected here would allow a ringed structure in the illumination profile, some were sufficiently narrow to follow quite closely the characteristics of a true monodispersion, except in the regions close to where the rings would occur The broad distributions, on the other hand, deviate from the monodispersion illumination profile, following below it for $\pi D_{32}\theta/\lambda < 3$ and above it for $\pi D_{32}\theta/\lambda > 3$ The cumulative effect of these trends produces the small total dispersion in the region noted previously

From the results, it is concluded that a value of D_{32} may be determined from the intensity of diffractively scattered light from a polydispersion of spherical particles to a good degree of accuracy for extremely wide ranges of distributions and without any knowledge of general distribution type It is felt that this conclusion appreciably extends the usefulness of the technique for measurement of mean particle size (D_{32}), especially since it may be used together with the results from a simple optical transmission test to determine particle concentration [1]

References

[1] Dobbins, R A Crocco, L , and Glassman, I , "Measurement of mean particle sizes of sprays from diffractively scattered light," AIAA J 1, 1882–1886 (1963)

[2] Mugele, R A and Evans, H D , "Droplet size distribution in sprays " Ind Eng Chem 43, 1317–1324 (1951)

[3] Deiss, W E , "The optical determination of particle sizes obeying the upper limit distribution function," Senior Thesis, Princeton Univ , Dept Aeronaut Eng (May 1960)

[4] Roberts, J H and Webb, M J , "The use of the upper limit distribution function in light scattering theory as applied to droplet diameter measurement," Princeton Univ , Eng Lab Rept 650 (1963)

Skip-Impact Criteria of a Re-Entry Trajectory with Negative Lift

CHARLES J RUGER*
Polytechnic Institute of Brooklyn, Freeport, N Y

Nomenclature

A = frontal area of re-entry body, ft^2
C_D = drag coefficient
C_L = lift coefficient
g = gravitational acceleration, ft/sec^2
h = altitude, ft
m = mass, slugs
r = distance from center of earth to re entry body, ft
t = time, sec
V = velocity, fps
W = weight, lb
β = constant in expression for exponential atmosphere 1/22,000, ft^{-1}
Δ = W/C_DA psf
θ = flight path angle, rad
ρ = atmospheric density, slug/ft^3

Subscripts

C = circular, critical
e = entry
m = minimum
s = sea level
$*$ = critical

FOR nonlifting re-entry trajectories it is known that if a nonlifting body re-enters the atmosphere with subcircular re-entry velocity the trajectory will be of the direct-impact type, whereas for a supercircular re-entry velocity the trajectory will be either a skip- or direct-impact type, depending on the values of the re-entry angle and velocity Kornreich[1] presents an approximate method for determining the re-entry conditions for a nonlifting body at which the trajectory changes from skip- to direct-impact type The skip-type trajectories mav be prevented by using enough negative lift to force a direct-impact trajectory This note presents an approximate method for determining the critical re-entry angle at which a trajectory switches from a skip- to a direct-impact type when given a re-entry velocity and a constant negative lift coefficient Three equations in three unknowns are presented along with an iteration procedure, which yields the value of the critical re-entry angle The latter is found to be in good agreement with values obtained by direct numerical integration of the equations of motion

The equation of motion along the direction of flight for a vehicle with aerodynamic forces is

$$\frac{d\theta}{dt} = -\frac{\rho V C_L A}{2m} + \left(\frac{g}{V} - \frac{V}{r}\right)\cos\theta \qquad (1)$$

Received December 18, 1963 This study was supported by the U S Air Force Office of Scientific Research Grant No AF-AFOSR 1 63 The author extends his thanks to Lu Ting for his guidance and encouragement in this work

* Research Fellow